JCB Article

Misfolding diverts CFTR from recycling to degradation: quality control at early endosomes

Manu Sharma,[1,2] Francesca Pampinella,[1,2] Csilla Nemes,[1,2] Mohamed Benharouga,[1,2] Jeffrey So,[1] Kai Du,[1] Kristi G. Bache,[4] Blake Papsin,[1] Noa Zerangue,[3] Harald Stenmark,[4] and Gergely L. Lukacs[1,2]

[1]Hospital for Sick Children Research Institute, Toronto, Ontario M5G 1X8, Canada
[2]Department of Laboratory Medicine and Pathobiology, University of Toronto, Toronto, Ontario M5G 1L5, Canada
[3]Howard Hughes Medical Institute, Department of Physiology and Biochemistry, University of California, San Francisco, San Francisco, CA 94143
[4]Department of Biochemistry, Institute for Cancer Research, The Norwegian Radium Hospital, Montebello, N-0310 Oslo, Norway

To investigate the degradation mechanism of misfolded membrane proteins from the cell surface, we used mutant cystic fibrosis transmembrane conductance regulators (CFTRs) exhibiting conformational defects in post-Golgi compartments. Here, we show that the folding state of CFTR determines the post-endocytic trafficking of the channel. Although native CFTR recycled from early endosomes back to the cell surface, misfolding prevented recycling and facilitated lysosomal targeting by promoting the ubiquitination of the channel. Rescuing the folding defect or down-regulating the E1 ubiquitin (Ub)-activating enzyme stabilized the mutant CFTR without interfering with its internalization. These observations with the preferential association of mutant CFTRs with Hrs, STAM-2, TSG101, hVps25, and hVps32, components of the Ub-dependent endosomal sorting machinery, establish a functional link between Ub modification and lysosomal degradation of misfolded CFTR from the cell surface. Our data provide evidence for a novel cellular mechanism of CF pathogenesis and suggest a paradigm for the quality control of plasma membrane proteins involving the coordinated function of ubiquitination and the Ub-dependent endosomal sorting machinery.

Introduction

Multiple quality control mechanisms are required to prevent the cellular accumulation and cytotoxicity of misfolded, aggregation-prone polypeptides (Sherman and Goldberg, 2001; Arvan et al., 2002; Ellgaard and Helenius, 2003). Newly synthesized soluble and membrane proteins that are unable to fold or assemble are targeted for proteolysis by the ER-associated degradation mechanism via the cytosolic ubiquitin (Ub)–proteasome system (Brodsky and McCracken, 1999; Hampton, 2002; Ellgaard and Helenius, 2003). In addition, nonnative membrane proteins are also recognized and targeted for lysosomal proteolysis directly from Golgi compartments (Wolins et al., 1997; Reggiori and Pelham, 2002). Yet, misfolded membrane proteins can escape these quality control checkpoints and reach the plasma membrane. Conformationally unstable plasma membrane proteins, such as unliganded MHC I and mutant variants of cystic fibrosis transmembrane conductance regulator (CFTR), α_2-receptors, α-factor receptor, and transferrin receptor, as well as influenza HA are rapidly degraded (Ljunggren et al., 1990; Li et al., 1999; Zaliauskiene et al., 2000; Benharouga et al., 2001; Sharma et al., 2001; Wilson et al., 2001; Fayadat and Kopito, 2003). Although a variety of sorting signals have been described to account for the constitutive or ligand-induced down-regulation of fully folded cell surface receptors and transporters (Rotin et al., 2000; Sorkin and Von Zastrow, 2002; Bonifacino and Traub, 2003; Hicke and Dunn, 2003), the molecular machinery that prevents the accumulation of misfolded plasma membrane proteins is not known in mammalian cells (Arvan et al., 2002).

The online version of this article includes supplemental material.

Address correspondence to Gergely L. Lukacs, Hospital for Sick Children, Program in Cell and Lung Biology, 555 University Ave., Toronto, Ontario M5G 1X8, Canada. Tel.: (416) 813-5125. Fax: (416) 813-5771. email: glukacs@sickkids.ca

Key words: recycling; sorting; mutation; endocytosis; ubiquitin receptors

Abbreviations used in this paper: CFTR, cystic fibrosis transmembrane conductance regulator; CHX, cycloheximide; ESCRT, endosomal sorting complex required for transport; Hrs, hepatocyte growth factor–regulated tyrosine kinase substrate; MVB, multivesicular body; STAM, signal-transducing adaptor molecule; Ub, ubiquitin; Vps, vacuolar protein sorting; wt, wild type.

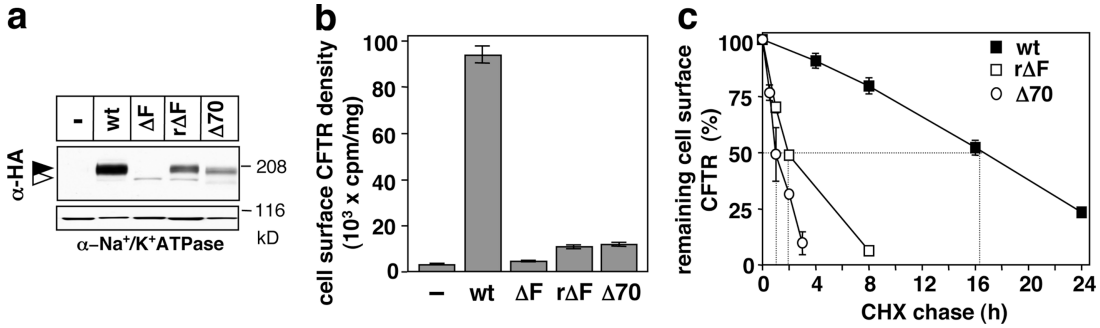

Figure 1. **Destabilizing mutations down-regulate CFTR from the plasma membrane.** For all experiments, rescued ΔF508 CFTR (rΔF508) was accumulated at 28°C for 24–36 h before the measurements. (a) Steady-state expression of CFTR variants. Equal amounts of cell lysates from BHK cells, expressing the indicated construct, were separated by SDS-PAGE. CFTR and Na^+/K^+-ATPase was visualized by immunoblotting with anti-HA and anti-Na^+/K^+-ATPase antibodies, respectively. Filled and empty arrowheads indicate the complex- and core-glycosylated CFTR, respectively. (b) The cell surface density of the CFTR variant was determined by anti-HA antibody and ^{125}I-conjugated secondary antibody binding at 0°C in BHK cells, and was normalized for cellular protein. Nonspecific antibody binding to mock-transfected BHK cells is indicated (-). (c) The turnover of cell surface resident wt, rΔF508, and Δ70 CFTR harboring the 3HA tag was monitored by their disappearance kinetics in the presence of 100 μg/ml CHX by the radioactive anti-HA antibody-binding assay at 37°C. Data are means ± SEM, $n = 2–4$. Similar results were obtained by monitoring the disappearance kinetics of prebound anti-HA antibody in the absence of CHX (not depicted).

Impaired plasma membrane expression or function of the CFTR, a cAMP-activated chloride channel, accounts for the phenotypic manifestation of CF, the most common inherited disorder in the Caucasian population (Zielenski and Tsui, 1995). Previously, we have identified two naturally occurring pathogenic mutants that display thermosensitive conformational defects in post-Golgi compartments. The COOH-terminally truncated CFTR, lacking the last 70 amino acid residues (Δ70 CFTR), traverses the biosynthetic pathway and undergoes complex glycosylation with the efficiency of wild-type (wt) CFTR (Haardt et al., 1999; Benharouga et al., 2001). In contrast, deletion of Phe508 (ΔF508, found in 90% of CF patients) imposes an ER processing block on CFTR that could be partially overcome or "rescued" at permissive temperature (<30°C) or by chemical chaperones in cultured cells (Denning et al., 1992; Sato et al., 1996). The conformational defect of the complex-glycosylated rescued ΔF508 (rΔF508) and the Δ70 CFTR has been demonstrated by their increased protease susceptibility, accounting for the four- to sixfold faster metabolic turnover of the mutants in post-Golgi compartments (Zhang et al., 1998; Benharouga et al., 2001; Sharma et al., 2001).

The present work was undertaken to elucidate the retrieval mechanism of conformationally defective Δ70 and rΔ508 CFTR from the cell surface that may represent a paradigm for the peripheral quality control of membrane proteins. The results suggest that misfolding of CFTR dramatically augments the ubiquitination susceptibility of the channel in post-Golgi compartments. In turn, Ub modification serves as a recognition signal for the Ub-dependent endosomal sorting machinery that reroutes the channel from recycling toward the multivesicular body (MVB)/lysosomal degradation.

Results

Misfolded CFTR is rapidly removed from the cell surface

Three tandem hemagglutinin (3HA) tags were engineered into the 4th extracellular loop of CFTR variants and expressed stably in BHK to monitor the cell surface density, internalization, and recycling rates of CFTR variants. The processing defect of the ΔF508 CFTR and the marked decrease in the expression level of mature, complex-glycosylated rΔF508 and Δ70 CFTR-3HA were in line with previous data obtained on untagged channel or on CFTR variants with NH_2- or COOH-terminal HA tags (Fig. 1 a; Haardt et al., 1999; Heda et al., 2001; Sharma et al., 2001). The rΔF508 and Δ70 CFTR have nearly 10-fold decreased cell surface density compared with their wt counterpart, measured by radioactive anti-HA antibody binding (Fig. 1 b), which can be, at least in part, attributed to their rapid disposal rates (Fig. 1 c). The cell surface half-life ($T_{1/2}$) of rΔF508 and Δ70 CFTR was ≈90% shorter ($T_{1/2} \approx 2$ h and ≈ 1 h, respectively) than that of the wt CFTR ($T_{1/2} \approx 16$ h), determined by the disappearance of anti-HA antibody binding in the presence of cycloheximide (CHX; Fig. 1c and Fig. S1, available at http://www.jcb.org/cgi/content/full/jcb.200312018/DC1). Similar results were obtained by monitoring the decay kinetics of bound anti-HA antibody in the absence of CHX (unpublished data).

To assess whether the rapid turnover of the mutants is due to their heterologous overexpression in BHK cells by itself, the biochemical and functional stability of the channel was measured in polarized pancreatic duct (PANC-1) and primary respiratory epithelia, representing a heterologous and an endogenous expression system, respectively. PANC-1 cells were chosen because the tightest genotype–phenotype correlation was established for the pancreatic manifestation of CF (Zielenski and Tsui, 1995). PANC-1 cells were stably transfected with the wt and ΔF508 CFTR. The biochemical turnover of the complex-glycosylated CFTR was measured by CHX- and brefeldin A-chase and immunoblotting on polarized monolayers. The turnover of rΔF508 was four- to fivefold faster than the wt form by both methods (Fig. 2, a and b). Comparable data were obtained for the functional stability of rΔF508 CFTR in the apical membrane, monitored by the iodide efflux assay (Fig. 2 c). Importantly, an even faster functional removal of the rΔF508 CFTR occurred from the

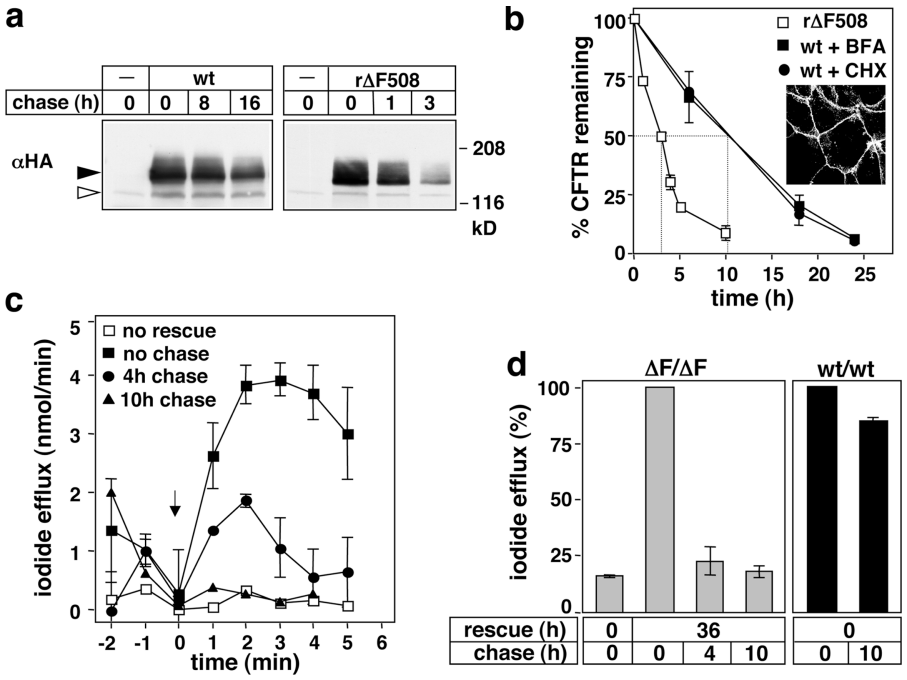

Figure 2. **Rescued ΔF508 CFTR (rΔF508) is unstable in polarized epithelia.** (a) Stably transfected PANC-1 cells were grown for >3 d at confluence, and then ΔF508 CFTR was rescued (at 26°C for 36 h). Disappearance of rΔF508 and wt CFTR was measured in the presence of 100 μg/ml CHX or 10 μg/ml brefeldin-A (not depicted) at 37°C by immunoblot analysis of equal amounts of cell lysates. Filled and empty arrowheads indicate the complex- and core-glycosylated CFTR, respectively. (b) Densitometric analysis of the disappearance of the complex-glycosylated wt and rΔF508 CFTR on immunoblots shown in a. Data are expressed as percentage of the initial amount and represent means ± SEM (n = 3–4). Inset: PANC-1 monolayer was immunostained for occludin to confirm polarization. (c) Functional stability of rΔF508 CFTR was measured by the iodide efflux assay in PANC-1 monolayers. The ΔF508 CFTR processing defect was rescued at 28°C (24 h) and the PKA-stimulated iodide release was measured after the indicated chase (0–10 h) at 37°C. (d) Functional turnover of rΔF508 and wt CFTR in differentiated respiratory epithelia derived from nasal polyps of homozygous (ΔF508/ΔF508) and healthy (wt/wt) individuals. The PKA-stimulated iodide release into the apical compartment on filter grown epithelia was monitored as a function of chase at 37°C after rescuing ΔF508 CFTR at 28°C for 36 h. Biosynthesis of wt CFTR was inhibited by 100 μg/ml CHX at 0 h.

apical plasma membrane of differentiated respiratory epithelia, obtained from nasal polyps of ΔF508/ΔF508 patients (Fig. 2 d and Fig. S2, available at http://www.jcb.org/cgi/content/full/jcb.200312018/DC1). The cAMP-stimulated iodide release, mediated by rΔF508 CFTR, almost completely disappeared after 4 h of chase at 37°C, whereas it remained unaltered in case of the wt CFTR (Fig. 2 d). These observations indicate that the metabolic instability of the rΔF508 CFTR is an inherent characteristic of the mutant and is independent of the expression system used.

Recycling of CFTR is inhibited by conformationally destabilizing mutations

Accelerated internalization, attenuated recycling, and/or facilitated targeting toward lysosomal degradation may account for the 10-fold decrease in the cell surface $T_{1/2}$ of the mutant CFTR. To distinguish between these possibilities, first the rate of CFTR endocytosis was measured by the disappearance of cell surface–bound anti-HA antibody. No significant difference could be resolved in the endocytosis rates of Δ70 CFTR (5.3 ± 0.7%/min, n = 3), rΔF508 (4.0 ± 1.4%/min, n = 3), and wt CFTR (4.9 ± 1.1%/min, n = 3) (Fig. 3 a).

To assess whether impaired recycling contributes to the reduced cell surface $T_{1/2}$, the exocytosis of internalized CFTR and anti-HA antibody complex was monitored with biotinylated secondary antibody and ^{125}I-labeled streptavidin. Although 63.2 ± 5.8% (n = 4) of internalized wt returned to the cell surface, only ≈6% of rΔF508 and Δ70 CFTR recycled in 10 min (Fig. 3 b). The recycling defect may constitute the primary cause of the decreased cell surface density and stability of the Δ70 CFTR (Fig. 1), suggesting a novel cellular mechanism for the severe clinical phenotype of patients with large COOH-terminal truncations (Haardt et al., 1999). Impaired recycling may also diminish the cell surface expression of the ΔF508 CFTR in selected CF tissues, where ER retention of the ΔF508 CFTR appears to be incomplete (Kalin et al., 1999).

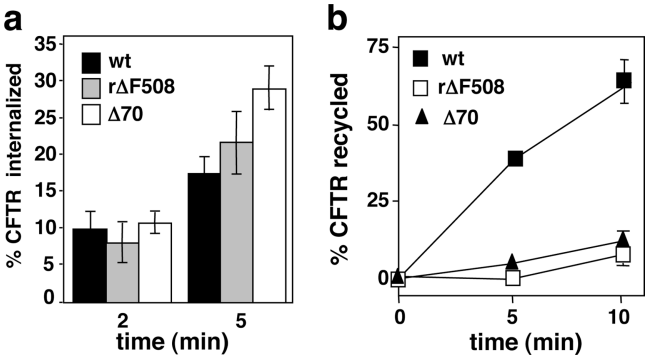

Figure 3. **Misfolding disrupts the constitutive recycling of CFTR.** (a) Endocytosis rates of the wt, rescued ΔF508 (rΔF508), and Δ70 CFTR were measured by antibody-capture assay in stably transfected BHK cells. CFTR-3HA variants were labeled with anti-HA antibody at 0°C, and the complex was internalized at 37°C. Antibody remaining at the cell surface was measured with ^{125}I-labeled secondary antibody. Data are expressed as percentage of the initial amount of specific antibody binding. (b) The recycling of wt, rΔF508, and Δ70 CFTR was measured after labeling the endosomal CFTR with anti-HA antibody at 37°C for 30 min, as described in the Materials and methods. After 5–10-min incubations at 37°C, recycled anti-HA–CFTR complexes were determined by biotinylated secondary antibody and ^{125}I-labeled streptavidin at 4°C. Recycling efficiency of CFTR is expressed as percentage of internalized anti-HA antibody, measured in parallel samples. Data are obtained from 3–4 independent experiments.

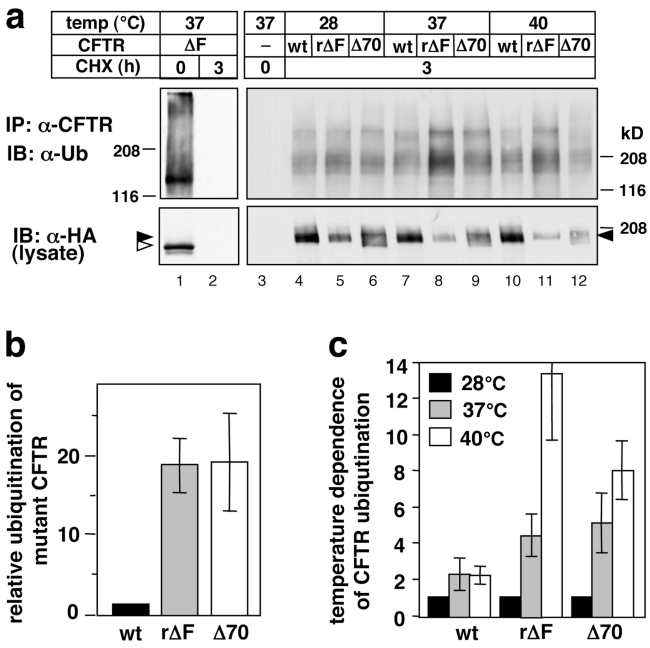

Figure 4. **Misfolding enhances the ubiquitination susceptibility of CFTR.** (a) Ub modification of wt, Δ70, and rΔF508 CFTR in post-Golgi compartments. Ubiquitinated core-glycosylated CFTR was eliminated by CHX chase (100 μg/ml, 3 h; lanes 2–12) in BHK cells. For the 28°C incubation, the CHX chase was performed at 37°C for 1 h and then at 28°C for 2 h. When indicated, cells were incubated at 37°C for 2 h and then at 40°C for 1 h. Solubilized CFTR was denatured in 2% SDS to avoid the isolation of irrelevant proteins. Then, CFTR was precipitated with the L12B4 anti-CFTR antibody. Immunoprecipitates were probed with anti-Ub antibody (FK2) and with visualized ECL (top). CFTR was visualized in the lysate with anti-HA antibody (bottom). Immunoprecipitates of both rΔF508 and Δ70 CFTR were obtained from 50 and 150% more cells at 37 and 40°C, respectively, than used for wt CFTR. Filled and empty arrowheads indicate the complex- and core-glycosylated form of CFTR, respectively. (b) Ubiquitination susceptibility of the rΔF508 and Δ70 relative to wt CFTR in post-Golgi compartments. Data are derived from densitometry of ubiquitinated CFTR shown in a, with apparent molecular mass including and larger than the complex-glycosylated CFTR. The abundance of ubiquitinated CFTR adducts was normalized for the expression level of their complex-glycosylated form and was expressed as fold increase relative to that of the wt CFTR. Data are means ± SEM, $n = 3$–4. (c) The temperature-dependent ubiquitination level of Δ70, rΔF508, and wt CFTR variants was measured as described in a and b. The level of ubiquitination for each construct is expressed as fold increase relative to that measured at 28°C.

Misfolding augments the ubiquitination of CFTR in post-Golgi compartments

Although nonnative soluble and ER-associated polypeptides are known substrates of ubiquitination, the susceptibility of poorly folded plasma membrane proteins to Ub conjugation is poorly understood. To assess whether Ub modification is involved in the disposal of nonnative CFTR, the ubiquitination level of wt and mutant CFTR, confined to post-Golgi compartments, was determined. To this end, complete degradation of the core-glycosylated ΔF508, Δ70, and wt CFTR (and their ubiquitinated adducts) was ensured by treating the cells with CHX for 3 h (Fig. 4 a, lanes 1 and 2, bottom and top, respectively; Fig. S3, available at http://www.jcb.org/cgi/content/full/jcb.200312018/DC1). Then, CFTR was immunoisolated under denaturing conditions with anti-CFTR antibody, and the precipitates were probed with anti-Ub antibody. Detection of ubiquitinated rΔF508, Δ70, and wt CFTR in cells expressing exclusively the complex-glycosylated forms by three different anti-Ub antibodies demonstrated that CFTR is susceptible to ubiquitination in post-Golgi compartments (Fig. 4 a; unpublished data). Importantly, densitometry showed that ubiquitination of the complex-glycosylated rΔF508 and Δ70 CFTR was increased by ≈20-fold relative to the wt channel at 37°C (Fig. 4 b).

To explore a possible correlation between the unfolding and the ubiquitination propensity of the channel, the conformation of CFTR variants was modulated by temperature shifts. Favoring the native conformation at the permissive temperature (28°C) attenuated the ubiquitination of the mutants, whereas promoting unfolding at 40°C substantially enhanced the ubiquitination of rΔF508 CFTR and moderately affected the Δ70 CFTR (Fig. 4 c). In contrast, ubiquitination of wt CFTR was virtually independent of the temperature (Fig. 4 c), suggesting that Ub conjugation may be involved in the degradation of conformationally unstable CFTR from post-Golgi compartments.

The CFTR-Ub chimera has recycling and stability defects

If Ub conjugation plays a primary role in the recycling and cell surface stability defect of the mutants, fusing Ub to the wt channel (CFTR-Ub) may mimic the consequences of destabilizing mutations. In-frame fusion of Ub to the COOH terminus of CFTR indeed inhibited the channel recycling by ≈90% (Fig. 5 a), reduced its cell surface $T_{1/2}$ from ≈16 to ≈1.3 h (Fig. 5 b), and diminished the steady-state expression of the mature CFTR (Fig. 5 c). These observations indicate that the chimera reproduces the peripheral trafficking defects of the rΔF508 and the Δ70 CFTR. Fusing a Ub molecule harboring arginines in place of all its lysine residues resulted in a similar expression and recycling defect to that of the CFTR-Ub (unpublished data), suggesting that the lysine residues of Ub do not serve as acceptor sites for poly-Ub chain formation in the chimera. The unaltered internalization rates of CFTR-Ub relative to wt CFTR (4.7 ± 1.3%/min; Fig. 5 d) is consistent with the notion that the Ub-dependent recycling defect is the primary cause for the rapid down-regulation of the chimera from the cell surface, as is for Δ70 and rΔ508 CFTR.

The activity of ubiquitination enzyme cascade is required for the endosomal sorting of misfolded CFTR toward lysosomal degradation

To substantiate the role of Ub conjugation in the degradation of the rΔF508 and Δ70 CFTR, we measured the cell surface stability of mutants in ts20 CHO cells, harboring the thermosensitive E1 Ub-activating enzyme. Consistent with the results of Kulka et al. (1988), the E1 enzyme was inactivated at 40°C in ts20 cells, whereas the expression level of the wt E1 remained unaltered in E36 cells, as shown by immunoblot analysis (Fig. 6 a). The disappearance kinetics of the mutant CFTR were determined by the radioactive antibody-binding assay after the inactivation of the E1 enzyme. Although inactivation of the E1 enzyme completely pre-

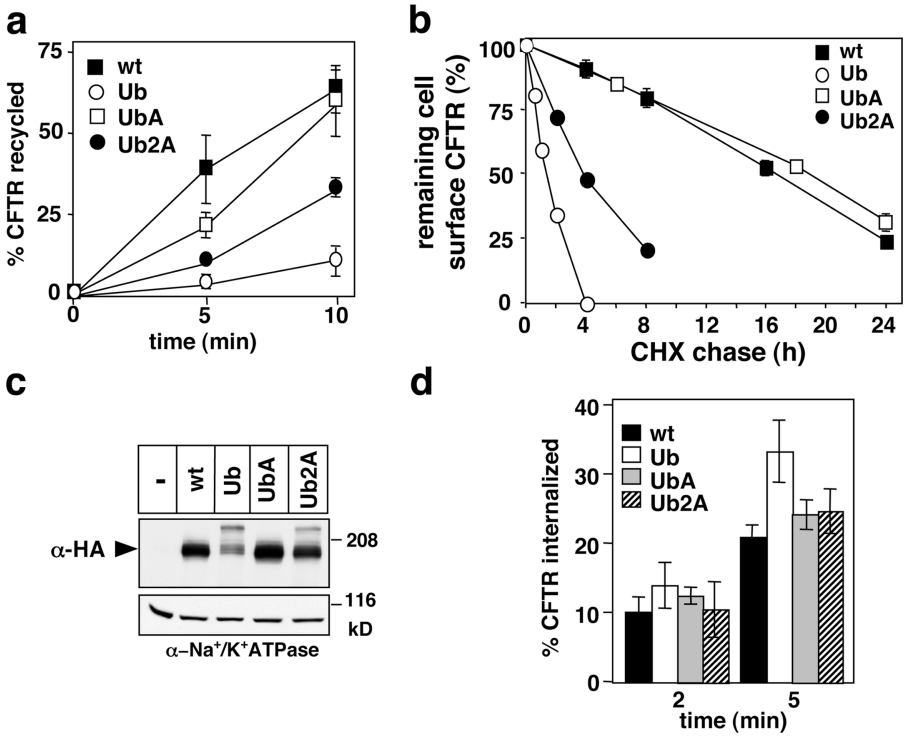

Figure 5. **The CFTR-Ub chimera mimics the peripheral trafficking defect of the misfolded CFTR.** (a) The recycling of CFTR (wt), CFTR-Ub (Ub), CFTR-UbA (UbA), and CFTR-Ub2A (Ub2A) was monitored by the biotin–streptavidin sandwich technique described in Fig. 3 b, in BHK cells stably expressing the respective construct. Data are means ± SEM, $n = 3$–4. (b) The cell surface stability of CFTR-Ub variants was determined by the anti-HA antibody-binding assay during the course of a CHX chase as in Fig. 1 c. (c) To determine the expression level of the CFTR variants, equal amount of lysates from BHK cells, expressing wt, CFTR-Ub, CFTR-UbA, and CFTR-Ub2A were separated by SDS-PAGE and probed with anti-HA antibody. The predominant complex-glycosylated forms are indicated by the filled arrowhead and have been verified by endoglycosidase H and peptide-*N*-glycanase F (not depicted). The origin of the lower mobility derivatives of CFTR is not known. (d) Endocytosis rates of CFTR, CFTR-Ub, CFTR-UbA, and CFTR-Ub2A chimeras were determined by the antibody-capture assay in BHK cells as described in Fig. 3 a.

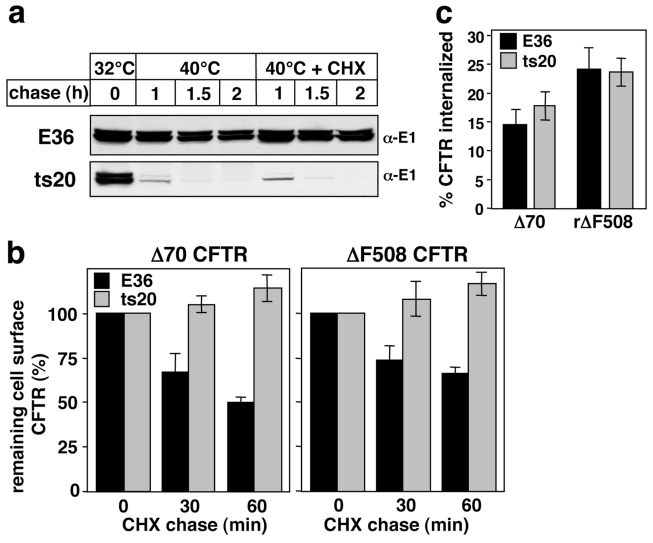

Figure 6. **The ubiquitination machinery is required for the disposal of misfolded CFTR by the endosomal sorting machinery.** (a) Down-regulation of the thermosensitive form and the wt E1 Ub-activating enzyme was monitored by immunoblotting the ts20 and E36 cells lysates, respectively, using anti-E1 antibody. Cells were lysed after shifting the culture temperature from 32 to 40°C. CHX does not influence the down-regulation of E1. (b) Stably transfected ts20 and E36 cells were incubated at 40°C for 1.5 h to down-regulate the E1 enzyme. Then, the cell surface density of Δ70 and rΔF508 CFTR was monitored by anti-HA antibody-binding assay in the presence of CHX. Data are means ± SEM ($n = 2$), performed in triplicate. (c) Internalization rates of Δ70 and rΔF508 CFTR were measured as described in Fig. 3 a after the incubation of ts20 and E36 cells at 40°C for 2 h to down-regulate the E1 enzyme.

vented the elimination of the rΔF508 and Δ70 CFTR from the cell surface in ts20 cells, the degradation of the mutants resumed in E36 cells (Fig. 6 b). Importantly, inactivation of the E1 enzyme had no effect on the internalization rates of the mutants in ts20 cells (Fig. 6 c).

Because the internalization rates of mutants are independent of E1 activity as well as the ubiquitination level of the CFTR variants (Fig. 3 a and Fig. 5 d), it is conceivable that Ub modification serves as a post-endocytic sorting signal for rerouting the mutant from recycling toward the MVB/lysosomal degradation pathway. Therefore, we tested the association of mutants with constituents of the Ub-dependent endosomal sorting machinery.

Association of misfolded CFTR and CFTR-Ub chimeras with the Ub-dependent endosomal sorting machinery

It is well established that targeting of certain ubiquitinated cell surface receptors for lysosomal degradation requires the recruitment of Ub-binding adaptor proteins (e.g., Hrs, STAM, and eps15, or their yeast orthologues Vps27, HSE1, and Ede1) to the cytosolic surface of early endosomes (Katzmann et al., 2002; Bonifacino and Lippincott-Schwartz, 2003). Because the hepatocyte growth factor–regulated tyrosine kinase substrate (Hrs) and signal-transducing adaptor molecule (STAM) are the primary Ub-interacting motif-containing adaptors that form the sorting complex involving components of the endosomal sorting complex required for transport I (ESCRT I; Bilodeau et al., 2002, 2003; Bishop et al., 2002; Katzmann et al., 2002; Raiborg et al., 2002; Shih et al., 2002; Mizuno et al., 2003; Schnell and Hicke, 2003),

the association of Hrs and STAM-2 with CFTR was assessed first. Immunoprecipitation of endogenous Hrs pulled down the complex-glycosylated rΔF508 and Δ70 CFTR as well as the CFTR-Ub, but neither the ER-associated ΔF508 CFTR nor the complex-glycosylated wt CFTR (Fig. 7 a). Selective association of STAM-2 (Fig. 7 b) and the TSG101 (Fig. 7 c), a component of ESCRT I, with the conformationally defective CFTR variants was also documented by the immunoprecipitation technique. Finally, similar results were obtained by probing for the association of CFTR variants with hVps25 and hVps32, components of the ESCRT II and III, respectively (Fig. 7 d). These observations are consistent with our hypothesis that the interaction of destabilized and preferentially ubiquitinated CFTR with the Ub-dependent sorting machinery is responsible for the recycling defect and accelerated degradation of the mutants.

To substantiate the inference that Ub-binding proteins have a role in rerouting misfolded CFTR from recycling to degradation, we took advantage of the observation that the hydrophobic surface of Ile_{44} in Ub is necessary for the association of Ub-binding proteins (Shih et al., 2002). If Ub recognition is required for rerouting the chimera, disrupting this interaction should reverse the trafficking defect. First, GST-Ub pull-down assays verified that Ile_{44}Ala mutation (UbA) abolished the Hrs binding to Ub, as observed for vacuolar protein sorting 27 (Vps27; Shih et al., 2002), whereas combining Ile_{44}Ala and Phe_4Ala caused partial inhibition (Fig. 7 e). The Phe_4Ala mutation was introduced to eliminate the endocytic signal of Ub (Shih et al., 2000). The Ile_{44}Ala alone (CFTR-UbA) or in combination with Phe_4Ala (CFTR-Ub2A) rescued the recycling (Fig. 5 a) and cell surface stability of the chimeras (Fig. 5 b). Consistently, the steady-state expression of CFTR-UbA and CFTR-Ub2A was significantly augmented (Fig. 5 c) without altering their internalization rates (Fig. 5 d). These data not only ruled out an indirect effect of Ub fusion, but also demonstrated that the recycling efficiency of ubiquitinated CFTR was dramatically attenuated by association with Ub-binding protein(s) of the endosomal sorting machinery. This was underscored by the observation that single Ala replacement prevented the association of Hrs as well as TSG101, Vps25, and Vps32 with the CFTR-UbA (Fig. 7, a–c).

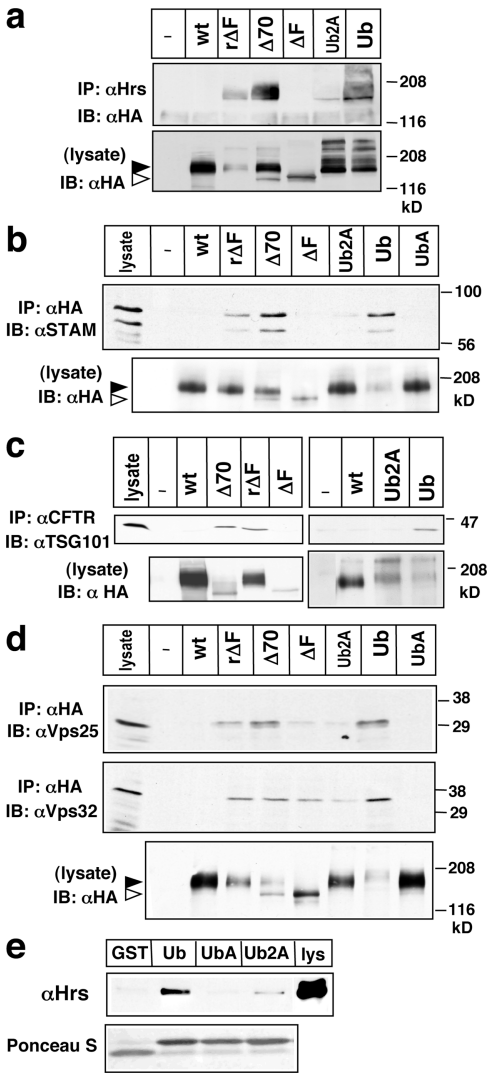

Figure 7. **Association of destabilized CFTR with the components of the Ub-dependent endosomal sorting machinery.** (a–c) Hrs, STAM-2, and TSG101 associate with destabilized CFTR in post-Golgi compartments. BHK cells expressing the indicated CFTR variant, except for Δ70 and ΔF508, were incubated in CHX for 3 h. Cells were lysed and Hrs was immunoprecipitated with anti-Hrs antibody. CFTR was visualized by anti-HA antibody. STAM-2 (b) and TSG101 (c) association was probed in the immunoprecipitates of CFTR with anti-TSG101 and anti-STAM-2 antibodies. (d) CFTR was immunoprecipitated with L12B4 and M3A7 anti-CFTR antibodies, and the complex was probed with anti-Vps25 and anti-Vps32 antibody. Considering the high abundance of wt CFTR, binding of the Vps is negligible to the wt form. (e) Hrs association with the indicated fusion protein; GST, GST-Ub (Ub), GST-UbF_4A (UbA), and GST-$UbF_4A,I_{44}A$ (Ub2A) was monitored by pull-down assay. Fusion proteins were incubated with HeLa cell lysate, protein complexes were isolated on glutathione-Sepharose, and the eluent was immunoblotted with rabbit anti-Hrs antibody (top). Fusion proteins were visualized by Ponceau S staining on the nitrocellulose membrane (bottom); lys, HeLa cell lysate. Filled and empty arrowheads indicate the complex- and core-glycosylated CFTR, respectively.

Rescuing the folding defect or preventing the Ub recognition restores the recycling of CFTR

To demonstrate the conformation-dependent endosomal sorting of CFTR, the subcellular destination of the mutants was determined as a function of the ambient temperature. CFTR containing endocytic compartments were identified based on their characteristic pH and protein composition (Mukherjee et al., 1997). Anti–mouse F_{ab} fragments conjugated to the pH-sensitive fluorophore FITC were complexed to anti-HA antibody and internalized with CFTR to measure the lumenal pH of CFTR-containing vesicles by ratiometric fluorescence video image analysis (Gagescu et al., 2000). Although recycling endosomes have a pH_{re} of 6.5 ± 0.05 and accumulate transferrin in BHK cells, the lysosomes have a pH_{ly} <5.0 (measured by FITC-EGF) and harbor LAMP-1 (Fig. 8 a and Fig. S4, available at http://www.jcb.org/cgi/content/full/jcb.200312018/DC1).

At physiological temperature (37°C), internalized wt CFTR was confined to endosomes with lumenal pH_{CFTR} of 6.5 ±

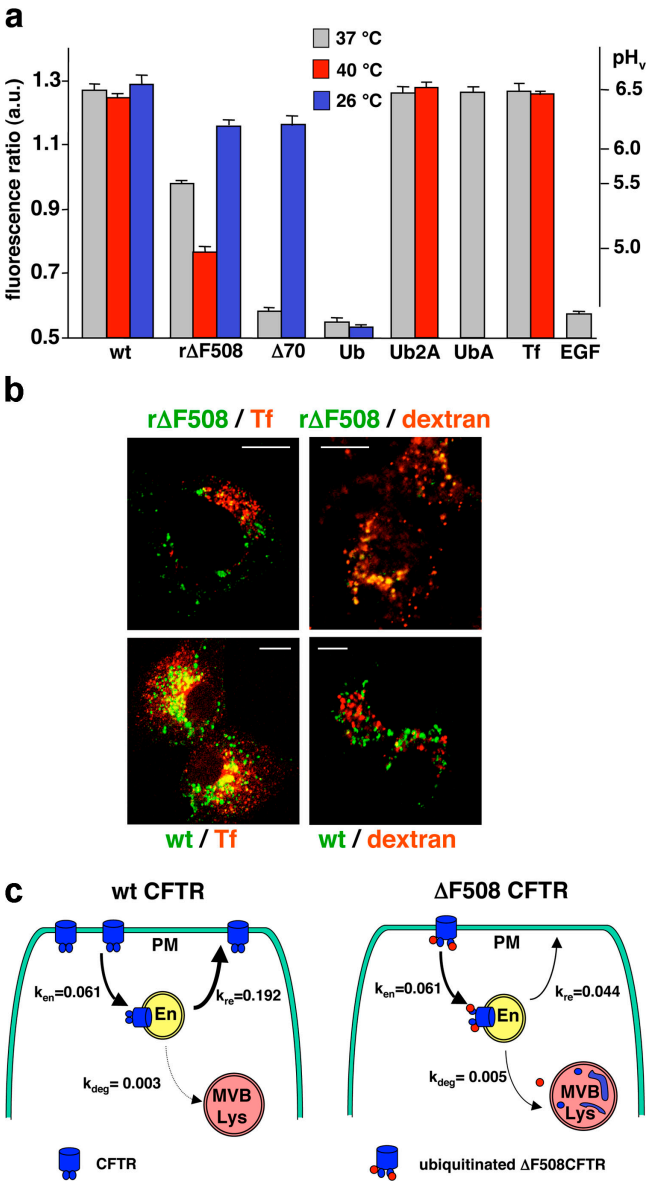

Figure 8. **Conformation-dependent sorting of CFTR in early endosomes.** (a) Monitoring the destination of internalized CFTR by organellar pH measurements. Ratiometric fluorescence video imaging of CFTR-containing vesicles in live cells was performed as described in the Materials and methods. Folding of mutants was facilitated by culturing the cells at 26°C for 1.5 h before internalization, whereas unfolding was promoted at 40°C. Internalization was performed for 3 h at 26 and 37°C and only for 1 h at 40°C. The pH of recycling endosome and lysosome was determined after the internalization of FITC-transferrin and FITC-EGF, respectively. The mean pH of vesicle populations was calculated by Origin software (Fig. S4). (b) BHK cells, expressing the 3HA-tagged rΔF508 or wt CFTR, were allowed to internalize monoclonal or polyclonal anti-HA antibody at 37°C for 3 h. Cells were fixed, permeabilized, and CFTR was colocalized with specific organellar markers. Recycling endosomes were labeled with Alexa Fluor® 598–transferrin (Tf). Lysosomes were visualized with TRITC-dextran by overnight labeling and subsequent chase for 3 h. Single optical sections of representative cells were obtained by fluorescence laser confocal microscopy. Bars, 10 μm. (c) Schematic model for the transport route of wt and rΔF508 CFTR from the cell surface. The recycling (k_{re}) and degradation (k_{deg}) rate constants were calculated by the SAAM II program (see Materials and methods) using the two-compartmental model, and were expressed as fractional transfer of molecules/min.

0.1 (Fig. 8 a and Fig. S4), a characteristic of recycling endosomes (Mukherjee et al., 1997). In contrast, the rΔF508 as well as the Δ70 CFTR were delivered to vesicles with lumenal pH typical of late endosomes and lysosomes ($pH_{\Delta F508}$ = 5.5 ± 0.05 and $pH_{\Delta 70}$ <5.0, respectively; Fig. 8 a), consistent with their rapid degradation (Fig. 1, b and c; Haardt et al., 1999; Benharouga et al., 2001). Attachment of Ub to CFTR efficiently diverted the channel from recycling endosomes into lysosomes with $pH_{CFTR\text{-}Ub}$ <5.0 ± 0.05, whereas preventing the recognition of Ub by the endosomal sorting machinery rerouted the CFTR-UbA and CFTR-Ub2A chimera to recycling endosomes ($pH_{CFTR\text{-}UbA}$ = 6.5 ± 0.02, $pH_{CFTR\text{-}Ub2A}$ = 6.5 ± 0.1; Fig. 8 a). Promoting unfolding of the rΔF508 CFTR at 40°C accelerated its delivery to more acidic vesicles ($pH_{r\Delta F508}$ = 5.0 ± 0.1) already within 1 h of internalization (Fig. 8 a). Conversely, at the permissive temperature where the native conformer was the predominant form, both rΔF508 and Δ70 CFTR were targeted to recycling endosomes with lumenal pH of 6.2 ± 0.05 and 6.19 ± 0.06, respectively (Fig. 8 a). These observations demonstrate the conformation-dependent sorting capacity of early endosomes. The targeting of the conformationally stable CFTR-Ub chimera to lysosomes and the wt CFTR-Ub2A and transferrin to recycling endosomes was insensitive to temperature shifts (Fig. 8 a).

Immunostaining of internalized CFTR variants with markers of recycling endosomes (transferrin) and lysosomes (FITC-dextran and Lamp-1) confirmed that internalized rΔF508 and Δ70 CFTR were diverted to MVB/lysosomes, whereas the wt CFTR was associated with recycling endosomes at 37°C (Fig. 8 b; unpublished data). Lysosomal proteolysis of the wt and Δ70 CFTR was also supported by the detection of immunoreactive degradation intermediates in purified lysosomes (Benharouga et al., 2001).

Kinetic model of CFTR peripheral trafficking

Besides sequestration of the mutant CFTR at the early endosomes, accelerated targeting into MVB/lysosomes could enhance the efficiency of the channel degradation (Katzmann et al., 2002; Hicke and Dunn, 2003). We used multicompartment kinetic analysis to estimate the intercompartmental transfer rates of the wt and rΔF508 channels. Endocytic rate constants (k_{en}) were calculated from the internalization rates. Based on k_{en}, turnover of the cell surface and the complex-glycosylated pools, degradation (k_{deg}), and recycling rate (k_{re}) constants were computed by the SAAM II multicompartment analysis program. The k_{deg} of the rΔF508 CFTR was increased by twofold relative to wt CFTR (Fig. 8 c). The k_{re} of rΔF508 CFTR was attenuated by nearly fivefold as compared with the wt (Fig. 8 c). These results, together with the recycling measurements, suggest that misfolding has a major impact on the sequestration of CFTR at early endosomes. Endosomal retention in concert with modestly accelerated transfer rates into MVB/lysosomal compartments is sufficient to attenuate the cell surface stability of the rΔF508 CFTR by 10-fold (Fig. 1 c).

Discussion

Major conformational defects account for the Ub-dependent degradation of newly synthesized wt and mutant

CFTR at ER (Kopito, 1999). Comparison of the ER and peripheral quality control of CFTR suggests that both processes entail three consecutive steps: the recognition of misfolded CFTR, the delivery of the channel to the relevant proteolytic machinery, and the proteolysis itself. Although substantial progress has been made in our understanding of membrane protein quality control at the ER (Cyr et al., 2002; Hampton, 2002; Ellgaard and Helenius, 2003; McCracken and Brodsky, 2003), the present work represents the first attempt to characterize the peripheral counterpart of this process in mammalian cells.

Misfolding promotes the ubiquitination of CFTR in post-Golgi compartments

Compelling evidence suggests that Ub conjugation is a prerequisite for the disposal of misfolded rΔF508 and Δ70 CFTR from the cell surface.

First, we demonstrated a correlation between the conformational destabilization and the ubiquitination propensity of rΔF508 and Δ70 CFTR in post-Golgi compartments. Rescuing the folding defect at the permissive temperature (28°C) diminished, whereas thermo-denaturation (40°C) further increased the ubiquitination of the mutants, leading to the preferential recycling or MVB/lysosomal targeting, respectively (Fig. 4 c). Neither accelerated biosynthesis nor the saturation of the degradation machinery can explain the nearly 20-fold increased level of ubiquitinated mutants as compared with that of the wt CFTR. The translational rates of the Δ70 and ΔF508 CFTR were comparable to that of the wt CFTR in BHK cells (Zhang et al., 1998; Haardt et al., 1999), and the copy number of wt CFTR at the cell surface is estimated to be only a few thousand molecules per cell.

Second, covalent attachment of Ub to the COOH-terminal tail of the wt CFTR reproduced the recycling as well as the cell surface stability defects of the mutants (Fig. 5). The genetically fused Ub mimics the cellular consequences of post-translational ubiquitination of CFTR rather than provoking misfolding. This conclusion is supported by the largely preserved processing efficiency of the CFTR-Ub (unpublished data), and the proportionally decreased PKA-stimulated whole-cell current and cell surface density of the chimera (Fig. S5, available at http://www.jcb.org/cgi/content/full/jcb.200312018/DC1). Furthermore, the $Ile_{44}Ala$ point mutation in Ub was able to restore the recycling and stability of the chimera to that of the wt CFTR (Fig. 5).

Finally, the most direct evidence for the role of Ub-conjugation was provided by the fact that heat inactivation of the E1 Ub-activating enzyme prevented the disappearance of Δ70 and rΔF508 CFTR from the plasma membrane in ts20 cells without influencing their endocytosis rates (Fig. 6). Collectively, these observations support the pivotal role of Ub modification in the down-regulation of the misfolded rΔF508 and Δ70 CFTR from the cell surface via post-endocytic mechanism(s).

Ubiquitination is known to effectively down-regulate receptors and transporters from the plasma membrane of yeast and mammalian cells (Rotin et al., 2000; Sorkin and Von Zastrow, 2002; Bonifacino and Traub, 2003; Hicke and Dunn, 2003). Ligand-induced (e.g., EGF and β-adrenergic agonist) or constitutive (e.g., ENaC) ubiquitination of membrane proteins requires substrate recognition by Ub-conjugating enzymes and Ub protein ligases (E2/E3s; Pickart, 2001). This process is usually mediated by protein–protein interaction domains of the relevant E3s (e.g., SH2, WW, and PDZ domains in Cbl, Nedd4/Rsp5, and LNX, respectively) and their cognate binding sites (e.g., phospho-Tyr, PPXY, phospho-Ser/Thr, or PDZ-binding motif; Weissman, 2001; Hicke and Dunn, 2003). Although it cannot be precluded that exposure of similar signals is involved in the ubiquitination of the two CFTR mutations, we favor the scenario that Ub conjugation is promoted by the unfolding of the channel and involves solvent-exposed hydrophobic protein surfaces. A similar mechanism has been invoked in the degradation of misfolded polypeptides at the ER (Laney and Hochstrasser, 1999; Cyr et al., 2002; Ellgaard and Helenius, 2003). Structural destabilization of the rΔF508 and Δ70 CFTR nucleotide-binding domains was indeed demonstrated (Zhang et al., 1998; Benharouga et al., 2001). This mechanism would also be reminiscent of the degradation signal identified in random peptides and in the Matα2 transcription factor (Sadis et al., 1995; Gilon et al., 1998, 2000; Johnson et al., 1998).

Importantly, a small amount of ubiquitinated wt, complex-glycosylated CFTR was reproducibly detected by three different anti-Ub antibodies (unpublished data). This cannot be attributed to the presence of other ubiquitinated polypeptides because CFTR was isolated under denaturing conditions. It is tempting to speculate that the low level of ubiquitination of the wt CFTR is caused by its slow, physiological unfolding that eventually terminates its long residence time ($T_{1/2} \approx 14$ h) at the cellular periphery. The profound difference in the metabolic turnover of protease-resistant, structurally stable wt and the protease-susceptible, conformationally labile mutant CFTR is consistent with the previously proposed hypothesis that the structural stability of soluble polypeptides constitutes one of the determinants of their metabolic stability (McLendon and Radany, 1978; Parsell and Sauer, 1989; Kowalski et al., 1998; Klink and Raines, 2000).

Misfolded CFTR is targeted toward lysosomal degradation by the Ub-dependent endosomal sorting machinery

Recycling of plasma membrane proteins protects polypeptides from degradation and allows them to undergo repeated cycles of endocytosis and exocytosis (Ghosh and Maxfield, 1995; Mellman, 1996). On the other hand, the sorting process at early endosomes offers an efficient mechanism to prevent the accumulation of misfolded membrane proteins at the cell surface. This is exemplified by the second step of the peripheral quality control of CFTR. Using Ub adducts of CFTR, obtained by post-translational ubiquitination or by genetic engineering, we presented three lines of evidence in support of the notion that ubiquitinated channels are selectively retrieved from recycling and are redirected for degradation into MVB/lysosomes. First, ubiquitination efficiently prevented the recycling and dramatically reduced the cell surface density, as well as the stability of the mutant and the chimera (Fig. 1 c, Fig. 3 b, and Fig. 5, a and b). Second, vesicular pH measurements verified that both the mutants and the CFTR-Ub are targeted

into lysosomes after their internalization, in contrast to the wt CFTR, which traverses recycling endosomes (Fig. 8 a). The recycling defect provides a plausible explanation for the 4–22-fold faster metabolic turnover rates of the rescued ΔF508 CFTR at 37 and 40°C, respectively (Sharma et al., 2001). Rescuing the folding defect and thus reducing the ubiquitination of the rΔF508 and Δ70 CFTR restored their constitutive recycling (Fig. 8 a) in parallel to their metabolic stabilization (Benharouga et al., 2001; Sharma et al., 2001). Third, immunocolocalization of endocytosed CFTR with markers of the recycling compartment and lysosomes substantiated the notion that the native and ubiquitinated CFTR are segregated at early endosomes (Fig. 8 b).

Ub-binding adaptor proteins, including Hrs and STAM, have a critical role in the retrieval of ubiquitinated cargo for lysosomal degradation at sorting endosomes (Raiborg et al., 2002; Sachse et al., 2002). Selective binding of destabilized rΔF508, Δ70 CFTR, and CFTR-Ub variants, but not the wt CFTR to Hrs, STAM-2, TSG101, Vps25, and Vps32, is consistent with the hypothesis that transport of ubiquitinated CFTR from early endosome to MVB/lysosomes involves its successive association with Hrs/STAM-2 and the human homologues of the ESCRT I, II, and III (Katzmann et al., 2002). Importantly, the $I_{44}A$ mutation in Ub not only prevented the recognition of CFTR-UbA and GST-UbA by Hrs and STAM-2, but also did so with downstream components of the ESCRT I, II, and III complexes (Fig. 7). As a result, CFTR-UbA resumed its constitutive recycling and escaped from MVB/lysosomal degradation (Fig. 5 b and Fig. 8 a), substantiating our working model that Ub recognition and the subsequent association of the misfolded CFTR with components of ESCRT complexes are required for MVB/lysosomal targeting.

Suppressor screens in yeast have identified several class E Vps mutants, including Vps23 and Vps27 (the yeast orthologues of TSG101 and Hrs, respectively), which are either directly or indirectly involved in the degradation of misfolded plasma membrane proteins (Li et al., 1999; Gong and Chang, 2001). Although the role of ubiquitination in the disposal of misfolded membrane proteins has not been established in yeast (Arvan et al., 2002), these observations suggest that some of the components of the peripheral quality control are evolutionarily conserved.

In summary, our analyses demonstrate that the folding state of CFTR is monitored not only during the early stage of its biogenesis in the ER (Brodsky and McCracken, 1999; Ellgaard et al., 1999; Arvan et al., 2002; Hampton, 2002), but is also surveyed in post-Golgi compartments. Our results provide direct evidence for the functional interplay between the ubiquitination machinery recognizing misfolded peripheral membrane proteins and the Ub-dependent endosomal sorting pathway in the elimination of misfolded CFTR, accounting for the cellular and clinical phenotype of the Δ70 CFTR mutation (Haardt et al., 1999). We propose that similar mechanisms may be involved in the recognition and degradation of other structurally destabilized membrane proteins that escape ER quality control or are generated by environmental stress. Thus, the peripheral quality control may have fundamental significance in the pathogenesis of conformational diseases and in the maintenance of cellular homeostasis.

Materials and methods

Expression of CFTR variants

BHK cells were stably transfected with wt, ΔF508, Δ70 CFTR, and the CFTR-Ub chimeras, harboring a single HA epitope at the NH_2 terminus (NHA; Haardt et al., 1999) or three tandem HA tags (3HA) in the 4th extracellular loop. After clonal selection in 500 μM methotrexate, 50–100 individual colonies were pooled and expanded for experiments. The HA tags preserved the biochemical and functional characteristics of CFTR (Haardt et al., 1999). Experiments have been performed on 3HA-tagged CFTR variants, if not indicated otherwise. Characterization of the 3HA-tagged CFTR will be described separately. PANC-1 cells (CRL1469; American Type Culture Collection) were stably transfected with the pMT/EP plasmid (provided by Dr. J. Ilan, Case Western Reserve University, Cleveland, OH) encoding the NHA-tagged wt or ΔF508 CFTR. Cells were seeded at confluence on plastic or on collagen-coated filters (Transwell-COL, 0.4-μm pore size; Costar) for iodide efflux and immunostaining. Differentiation was ensured by culturing the epithelia for more than three additional days. Expression of CFTR was induced by 50 μM $ZnSO_4$. CFTR-expressing ts20 and E36 cell lines were generated by retroviral infection (Benharouga et al., 2003). CFTR-Ub was constructed by fusing Ub in frame to the COOH terminus of CFTR using PCR (Shih et al., 2000). Mutant chimeras, incorporating $UbF_4A,I_{44}A$ (CFTR-Ub2A), $UbI_{44}A$ (CFTR-UbA), and the Lys-less Ub were generated by PCR mutagenesis. The cDNA of Lys-less Ub was provided by Dr. L. Hicke (Northwestern University, Evanston, IL). Similar expression levels of the CFTR chimeras were observed regardless whether CFTR harbored the NHA or the 3HA epitope.

Expression of recombinant Ub for pull-down assay

Bacterial expression plasmids containing GST-Ub, GST-$UbF_4A,I_{44}A$ (GST-Ub2A), and GST-UbF_4A (GST-UbA) were constructed by PCR mutagenesis in pGEX4T, and were expressed in HB101 cells. Recombinant proteins were purified, bound to glutathione-sepharose 4B (Amersham Biosciences), and incubated with HeLa cell lysate (3 mg, at 4°C for 2 h). Bound polypeptides were separated by SDS-PAGE and Hrs was visualized by immunoblotting with a polyclonal anti-Hrs antibody (Raiborg et al., 2002).

Cultures of differentiated human primary respiratory epithelia

Nasal polyps were obtained from surgical materials of CF and non-CF individuals with informed consent of the family by a procedure approved by the Research Ethics Board of the Hospital for Sick Children. Two of the CF patients were homozygous ΔF508, and the third one had ΔF508/R1162X genotype. Explants were grown on collagen-coated dishes in DME/Ham's F12, 20% FBS, gentamycin, streptomycin, and amphotericin-B. Fibroblasts were removed by trypsinization, and epithelial cells were seeded at >80% confluence on collagen-coated filters and were cultured for >3 d. Polarization was demonstrated by the domain-specific CFTR-mediated anion conductance (Fig. S1 a).

Immunoblotting, immunoprecipitation, and electrophysiology

Immunoblotting of CFTR and densitometric analysis was performed with NIH image 1.62 as described previously using ECL (Sharma et al., 2001). Antibodies were used as follows: FK1, FK2 (Affinity BioReagents, Inc.), and P4D1 (Santa Cruz Biotechnology, Inc.) anti-Ub antibodies; a6F anti-Na/K ATPase antibody (Developmental Studies Hybridoma Bank, University of Iowa, Iowa city, IA), M3A7 and L12B4 anti-CFTR antibody (Chemokine) and a rabbit polyclonal anti-CFTR antibody raised against the COOH-terminal tail of CFTR; 4A10 anti-TSG101 antibody (GeneTex); and anti-Hrs (Raiborg et al., 2002) and anti-E1 enzyme antibodies (Covance). Rabbit pAbs against human Vps25/EAP25 and human Vps32/CHMP4B were raised against maltose-binding protein fusion proteins and were affinity purified on Affi-Gel beads (Bio-Rad Laboratories) containing recombinant proteins. Whole-cell current measurements were performed as described previously (Haardt et al., 1999).

Cell surface density measurements, internalization, and recycling of CFTR

The cell surface density of 3HA-tagged CFTR was measured by the binding of the monoclonal anti-HA antibody (Covance; at 0°C for 1 h) and ^{125}I-labeled goat anti–mouse secondary antibody (3 μCi/ml, at 0°C for 1 h; Amersham Biosciences). Specific binding was calculated by correcting with the nonspecific antibody adsorption in the presence of 10 μg/ml nonimmune IgG (Santa Cruz Biotechnology, Inc.). Nonspecific antibody binding was usually 3–5% of the specific signal. Internalization of CFTR was calculated from the removal rate of anti-HA antibody from the cell surface during 2–5-min internalization at 37°C. Data are expressed as percentage of the specific radioactivity detected before internalization.

To measure CFTR recycling, first the endosomal CFTR was labeled with anti-HA antibody (at 37°C for 30 min). Then the remaining cell surface–associated antibody was blocked by biotinylated goat anti–mouse antibody (KPL) and 10 μg/ml streptavidin (Sigma-Aldrich) on ice. Recycling was initiated by shifting the temperature to 37°C for 5–10 min. The amount of exocytosed antibody–CFTR complex was measured by biotinylated secondary antibody and ^{125}I-streptavidin (Amersham Biosciences) at 0°C, and was expressed as the percentage of the anti-HA antibody associated with the endosomal compartment before exocytosis. The internalized anti-HA antibody in complex with CFTR was determined in parallel by monitoring the disappearance of cell surface anti-HA antibody with the biotin–streptavidin sandwich technique. The internalized anti-HA antibody was corrected for the degradation of mutant CFTR during the labeling. The radioactivity corresponding to internalized anti-HA antibody was ≈40,000 and ≈10,000–20,000 cpm for the wt and mutants, respectively. Each data point represents 3–4 independent experiments, consisting of triplicate measurements.

Vesicular pH measurement of CFTR-containing endocytic organelles

The pH of endocytic vesicles containing CFTR was measured by fluorescence ratio imaging of internalized anti-HA antibody (Covance) complexed with FITC-conjugated goat anti–mouse F_{ab} antibody (Jackson ImmunoResearch Laboratories). Cells were incubated with the primary and secondary antibodies in tissue culture medium at 37°C for 1–3 h, washed with NaKH medium (140 mM NaCl, 5 mM KCl, 20 mM Hepes, 10 mM glucose, 0.1 mM $CaCl_2$, and 1 mM $MgCl_2$, pH 7.3), and imaged on a microscope (Axiovert 100; Carl Zeiss MicroImaging, Inc.) at 35°C, equipped with a cooled CCD camera (Princeton Instruments) and a 63× NA 1.4 Planachromat objective. The metabolic stability of CFTR was not influenced by the continuous presence of anti-HA primary and secondary antibody (Fig. S2), indicating that antibody binding did not promote the degradation of CFTR.

Image acquisition and analysis were performed with the MetaFluor® software (Universal Imaging Corp.). Images were acquired at 490 ± 5 nm, and 440 ± 10 nm excitation wavelength, using a 535 ± 25 nm emission filter. In situ calibration curves were obtained by clamping the vesicular pH between 4.5 and 7.0 in K^+-rich medium (135 mM KCl, 10 mM NaCl, 20 mM Hepes or 20 mM MES, 1 mM $MgCl_2$, and 0.1 mM $CaCl_2$, containing 10 μM nigericin, 10 μM monensin, and 5 μM carbonyl cyanide *p*-chlorophenylhydrazon) and recording the fluorescence ratio of cells loaded with FITC-transferrin (Molecular Probes, Inc.), FITC-EGF (followed by a 2-h chase), or FITC-F_{ab} and anti-HA antibody in CFTR-Ub2A expressors. The fluorescence ratios as a function of extracellular pH provided the standard curve for the pH determination of CFTR-containing endosome. In addition, one point calibration was done on each coverslip by clamping the vesicular pH to 6.5. Mono- and multi-peak Gaussian fits for vesicular pH were performed with Origin 7.0 software (OriginLab® Corporation). The average pH of each type of vesicle population was calculated as the arithmetic mean of the data and was identical to the Gaussian mean, based on single-peak distribution fitting, except for Δ70 CFTR, where two-peak Gaussian distribution analysis was done (Fig. S4).

Kinetic modeling of wt and rΔF508 CFTR trafficking

The recycling (k_{re}) and degradation (k_{deg}) rate constants of CFTR were calculated by the SAAM II program (University of Washington, Seattle, WA), using a two-compartmental model (Fig. 8 c) and the Rosenbrock integration method. Data for fitting were obtained from the cell surface decay kinetics of wt and rΔF508 CFTR complexed to anti-HA antibody. The value of k_{de} was adjusted so that the model reproduced metabolic half-life of the complex-glycosylated rΔF508 and wt CFTR measured by the pulse-chase technique (Sharma et al., 2001). It was assumed that degradation of CFTR in the MVB/lysosomes is instantaneous. The rate constants are expressed as fractional transfer of molecules/min.

Statistical analysis

Experiments were repeated at least three times, and graphs include means ± SEM. Two-tailed P values were calculated at 95% confidence level with unpaired *t* test, using Prism software (GraphPad Software, Inc.).

Online supplemental material

Fig. S1 demonstrates that anti-HA antibody binding does not induce degradation of the wt CFTR. Fig. S2 illustrates the functional polarization of human respiratory epithelia. Elimination of the core-glycosylated CFTR during the CHX chase is documented in Fig. S3. Fig. S4 shows the pH distribution curves of vesicles containing CFTR variants. The electrophysiological characterization of the CFTR-Ub chimera is depicted in Fig. S5. Online supplemental material available at http://www.jcb.org/cgi/content/full/jcb.200312018/DC1.

We are grateful to J. Gruenberg, L. Hicke, J. Ilan, and R. Haguenauer-Tsapis for providing anti-Lamp1 antibody and plasmid DNAs. We thank J. Rommens and R. Reithmeier for helpful comments, and L. Drzymala and M. Popov for the construction of CFTR-Ub chimeras.

M. Benharouga was supported by a Canadian Institutes of Health Research (CIHR) postdoctoral fellowship. J. So was awarded a summer studentship from the Canadian Cystic Fibrosis Foundation (CCFF). This work was supported by grants from CCFF and the CIHR to G.L. Lukacs. H. Stenmark was supported by the Research Council of Norway, the Novo Nordisk Foundation, and the Norwegian Cancer Society. M. Sharma is a CIHR doctoral student. F. Pampinella is a postdoctoral fellow of the CCFF.

Submitted: 3 December 2003
Accepted: 29 January 2004

References

Arvan, P., X. Zhao, J. Ramos-Castaneda, and A. Chang. 2002. Secretory pathway quality control operating in Golgi, plasmalemmal, and endosomal systems. *Traffic.* 3:771–780.

Benharouga, M., M. Haardt, N. Kartner, and G.L. Lukacs. 2001. COOH-terminal truncations promote proteasome-dependent degradation of mature cystic fibrosis transmembrane conductance regulator from post-Golgi compartments. *J. Cell Biol.* 153:957–970.

Benharouga, M., M. Sharma, J. So, M. Haardt, L. Drzymala, M. Popov, B. Schwapach, S. Grinstein, K. Du, and G.L. Lukacs. 2003. The role of the C terminus and Na^+/H^+ exchanger regulatory factor in the functional expression of cystic fibrosis transmembrane conductance regulator in nonpolarized cells and epithelia. *J. Biol. Chem.* 278:22079–22089.

Bilodeau, P., J. Urbanowski, S. Winistorfer, and R. Piper. 2002. The Vps27p Hse1p complex binds ubiquitin and mediates endosomal protein sorting. *Nat. Cell Biol.* 4:534–539.

Bilodeau, P., S. Winistorfer, W. Kearney, A. Robertson, and R. Piper. 2003. Vps27-Hse1 and ESCRT-I complexes cooperate to increase efficiency of sorting ubiquitinated proteins at the endosome. *J. Cell Biol.* 163:237–243.

Bishop, N., A. Horman, and P. Woodman. 2002. Mammalian class E vps proteins recognize ubiquitin and act in the removal of endosomal protein-ubiquitin conjugates. *J. Cell Biol.* 157:91–101.

Bonifacino, J., and J. Lippincott-Schwartz. 2003. Coat proteins: shaping membrane transport. *Nat. Rev. Mol. Cell Biol.* 4:409–414.

Bonifacino, J., and L. Traub. 2003. Signals for sorting of transmembrane proteins to endosomes and lysosomes. *Annu. Rev. Biochem.* 72:395–447.

Brodsky, J.L., and A.A. McCracken. 1999. ER protein quality control and proteasome-mediated protein degradation. *Semin. Cell Dev. Biol.* 10:507–513.

Cyr, D., J. Hohfeld, and C. Patterson. 2002. Protein quality control: U-box-containing E3 ubiquitin ligases join the fold. *Trends Biochem. Sci.* 27:368–375.

Denning, G.M., M.P. Anderson, J.F. Amara, J. Marshall, A.E. Smith, and M.J. Welsh. 1992. Processing of mutant cystic fibrosis transmembrane conductance regulator is temperature-sensitive. *Nature.* 358:761–764.

Ellgaard, L., and A. Helenius. 2003. Quality control in the endoplasmic reticulum. *Nat. Rev. Mol. Cell Biol.* 4:181–191.

Ellgaard, L., M. Molinari, and A. Helenius. 1999. Setting the standards: quality control in the secretory pathway. *Science.* 286:1882–1888.

Fayadat, L., and R. Kopito. 2003. Recognition of a single transmembrane degron by sequential quality control checkpoints. *Mol. Biol. Cell.* 14:1268–1278.

Gagescu, R., N. Demaurex, R. Parton, W. Hunziker, L. Huber, and J. Gruenberg. 2000. The recycling endosome of MDCK cells is a mildly acidic compartment rich in raft components. *Mol. Biol. Cell.* 11:2775–2791.

Ghosh, R.N., and F.R. Maxfield. 1995. Evidence for nonconventional, retrograde transferrin trafficking in the early endosomes of HEp2 cells. *J. Cell Biol.* 128: 549–561.

Gilon, T., O. Chomsky, and R.G. Kulka. 1998. Degradation signals for ubiquitin system proteolysis in *Saccharomyces cerevisiae. EMBO J.* 17:2759–2766.

Gilon, T., O. Chomsky, and R. Kulka. 2000. Degradation signals recognized by the Ubc6p-Ubc7p ubiquitin-conjugating enzyme pair. *Mol. Cell. Biol.* 20: 7214–7219.

Gong, X., and A. Chang. 2001. A mutant plasma membrane ATPase, Pma1-10, is

defective in stability at the yeast cell surface. *Proc. Natl. Acad. Sci. USA.* 98: 9104–9109.

Haardt, M., M. Benharouga, D. Lechardeur, N. Kartner, and G. Lukacs. 1999. C-terminal truncations destabilize the CFTR without impairing its biogenesis. A novel class of mutation. *J. Biol. Chem.* 274:21873–21877.

Hampton, R. 2002. ER-associated degradation in protein quality control and cellular regulation. *Curr. Opin. Cell Biol.* 14:476–482.

Heda, G., M. Tanwani, and C. Marino. 2001. The ΔF508 mutation shortens the biochemical half-life of plasma membrane CFTR in polarized epithelial cells. *Am. J. Physiol. Cell Physiol.* 280:C166–C174.

Hicke, L., and R. Dunn. 2003. Regulation of membrane protein transport by ubiquitin and ubiquitin-binding proteins. *Annu. Rev. Cell Dev. Biol.* 19:141–172.

Johnson, P.R., R. Swanson, L. Rakhilina, and M. Hochstrasser. 1998. Degradation signal masking by heterodimerization of MATα2 and MATa1 blocks their mutual destruction by the ubiquitin-proteasome pathway. *Cell.* 94:217–227.

Kalin, N., A. Claas, M. Sommer, E. Puchelle, and B. Tummler. 1999. Δ508CFTR protein expression in tissues from patient with cystic fibrosis. *J. Clin. Invest.* 103:1379–1389.

Katzmann, D., G. Odorizzi, and S. Emr. 2002. Receptor downregulation and multivesicular-body sorting. *Nat. Rev. Mol. Cell Biol.* 3:893–905.

Klink, T., and R. Raines. 2000. Conformational stability is a determinant of ribonuclease A cytotoxicity. *J. Biol. Chem.* 275:17463–17467.

Kopito, R.R. 1999. Biosynthesis and degradation of CFTR. *Physiol. Rev.* 79:S163–S173.

Kowalski, J., R. Parekh, J. Mao, and K. Wittrup. 1998. Protein folding stability can determine the efficiency of escape from endoplasmic reticulum quality control. *J. Biol. Chem.* 273:19453–19458.

Kulka, R., B. Raboy, R. Schuster, H. Parag, G. Diamond, A. Ciechanover, and M. Marcus. 1988. A Chinese hamster cell cycle mutant arrested at G2 phase has a temperature-sensitive ubiquitin-activating enzyme, E1. *J. Biol. Chem.* 263: 15726–15731.

Laney, J.D., and M. Hochstrasser. 1999. Substrate targeting in the ubiquitin system. *Cell.* 97:427–430.

Li, Y., T. Kane, C. Tipper, P. Spatrick, and D. Jennes. 1999. Yeast mutants affecting possible quality control of plasma membrane proteins. *Mol. Cell. Biol.* 19:3588–3599.

Ljunggren, H., N. Stam, C. Ohlen, J. Neefjes, P. Hoglund, M. Heemels, J. Bastin, T. Schumacher, A. Townsend, K. Karre, and H. Ploegh. 1990. Empty MHC class I molecules come out in the cold. *Nature.* 346:476–480.

McCracken, A., and J. Brodsky. 2003. Evolving questions and paradigm shifts in endoplasmic-reticulum-associated degradation (ERAD). *Bioessays.* 25:868–877.

McLendon, G., and E. Radany. 1978. Is protein turnover thermodynamically controlled? *J. Biol. Chem.* 253:6335–6337.

Mellman, I. 1996. Endocytosis and molecular sorting. *Annu. Rev. Cell Dev. Biol.* 12:575–625.

Mizuno, E., K. Kawahata, M. Kato, N. Kitamura, and M. Komada. 2003. STAM proteins bind ubiquitinated proteins on the early endosome via the VHS domain and ubiquitin-interacting motif. *Mol. Biol. Cell.* 14:3675–3689.

Mukherjee, S., R. Ghosh, and F. Maxfield. 1997. Endocytosis. *Physiol. Rev.* 77: 759–803.

Parsell, D., and R. Sauer. 1989. The structural stability of a protein is an important determinant of its proteolytic susceptibility in *Escherichia coli*. *J. Biol. Chem.* 264:7590–7595.

Pickart, C. 2001. Mechanism underlying ubiquitination. *Annu. Rev. Biochem.* 70: 503–533.

Raiborg, C., K.G. Bache, D.J. Gillooly, I.H. Madshus, E. Stang, and H. Stenmark. 2002. Hrs sorts ubiquitinated proteins into clathrin-coated microdomains of early endosomes. *Nat. Cell Biol.* 4:394–398.

Reggiori, F., and H. Pelham. 2002. A transmembrane ubiquitin ligase required to sort membrane proteins into multivesicular bodies. *Nat. Cell Biol.* 4:117–123.

Rotin, D., O. Staub, and R. Haguenauer-Tsapis. 2000. Ubiquitination and endocytosis of plasma membrane proteins: role of Nedd4/Rsp5 family of ubiquitin-protein ligases. *J. Membr. Biol.* 176:1–17.

Sachse, M., S. Urbe, V. Oorschot, G.J. Strous, and J. Klumperman. 2002. Bilayered clathrin coats on endosomal vacuoles are involved in protein sorting toward lysosomes. *Mol. Biol. Cell.* 13:1313–1328.

Sadis, S., C.J. Atienza, and D. Finley. 1995. Synthetic signals for ubiquitin-dependent proteolysis. *Mol. Cell. Biol.* 15:4086–4094.

Sato, S., C. Ward, M. Krouse, J. Wine, and R. Kopito. 1996. Glycerol reverses the misfolding phenotype of the most common cystic fibrosis mutation. *J. Biol. Chem.* 271:635–638.

Schnell, J., and L. Hicke. 2003. Non-traditional functions of ubiquitin and ubiquitin-binding proteins. *J. Biol. Chem.* 278:35857–35860.

Sharma, M., M. Benharouga, W. Hu, and G.L. Lukacs. 2001. Conformational and temperature-sensitive stability defects of the delta F508 cystic fibrosis transmembrane conductance regulator in post-endoplasmic reticulum compartments. *J. Biol. Chem.* 276:8942–8950.

Sherman, M., and A. Goldberg. 2001. Cellular defenses against unfolded proteins: a cell biologist thinks about neurodegenerative diseases. *Neuron.* 29:15–32.

Shih, S.C., K.E. Sloper-Mould, and L. Hicke. 2000. Monoubiquitin carries a novel internalization signal that is appended to activated receptors. *EMBO J.* 19: 187–198.

Shih, S., D. Katzmann, J. Schnell, M. Sutanto, S. Emr, and L. Hicke. 2002. Epsins and Vps27p/Hrs contain ubiquitin-binding domains that function in receptor endocytosis. *Nat. Cell Biol.* 4:389–393.

Sorkin, A., and M. Von Zastrow. 2002. Signal transduction and endocytosis: close encounters of many kinds. *Nat. Rev. Mol. Cell Biol.* 3:600–614.

Weissman, A.M. 2001. Themes and variations on ubiquitylation. *Nat. Rev. Mol. Cell Biol.* 2:169–178.

Wilson, M., H. Highfield, and L. Limbird. 2001. The role of a conserved intertransmembrane domain interface in regulating α_{2a}-adrenergic receptor conformational stability and cell-surface turnover. *Mol. Pharmacol.* 59:929–938.

Wolins, N., H. Bosshart, H. Kuster, and J.S. Bonifacino. 1997. Aggregation as a determinant of protein fate in post-Golgi compartments: role of the luminal domain of furin in lysosomal targeting. *J. Cell Biol.* 139:1735–1745.

Zaliauskiene, L., S. Kang, C. Brouillette, J. Lebowitz, R. Arani, and J. Collawn. 2000. Down-regulation of cell surface receptors is modulated by polar residues within the transmembrane domain. *Mol. Biol. Cell.* 11:2643–2655.

Zhang, F., F. Kartner, and G.L. Lukacs. 1998. Limited proteolysis as a probe for arrested conformational maturation of the ΔF508 CFTR. *Nat. Struct. Biol.* 5:180–183.

Zielenski, J., and L.-C. Tsui. 1995. Cystic fibrosis: genotypic and phenotypic variations. *Annu. Rev. Genet.* 29:777–807.